Mössbauer relaxation studies of ^{170}Yb in dilute Au : ^{170}Tm sources in external magnetic fields up to 55 kG

J. Stöhr
Physik-Department, Technische Universität München, 8046 Garching, Germany
(Received 10 June 1974)

Relaxation effects of Yb impurities in Au have been studied by Mössbauer-source experiments at both 4.2 K in external magnetic fields ranging from 10 to 55 kG, and at 50 kG in the temperature range 4.2 to 40 K. In order to analyze the results a general microscopic relaxation theory for an effective-field hyperfine interaction is derived, which allows for both a generalized tensor-type $4f$ conduction-electron coupling, and frequency-dependent relaxation processes between the electronic energy levels. It is pointed out that in Mössbauer-source experiments the preceeding nuclear β decay may produce population effects in the lowest electronic energy states due to slow relaxation rearrangement in the electronic shell. The experimental Mössbauer spectra of ^{170}Yb in dilute Au : ^{170}Tm sources are found to be well described by the relaxation theory including the new rearrangement ideas for Mössbauer-source experiments.

I. INTRODUCTION

The hyperfine (hf) structure of a $3d$ impurity in a nonmagnetic metal is usually not observed because of fast relaxation processes between the electronic energy levels.[1] However, in the presence of an external magnetic field a polarization of the electronic moment results and a hf structure may be observed. The situation for rare-earth (RE) impurities in metals is quite different. Electronic relaxation times are typically two orders of magnitude longer and nuclear correlation times an order of magnitude shorter than for $3d$ elements. This leads to a well-resolved paramagnetic hf structure at temperatures around 4.2 K.[2-6] In the case of $4f$ elements the application of an external magnetic field is then only an additional possibility in the study of the hf structure and relaxation effects.

In a previous paper[7] we have reported a Mössbauer-effect (ME) study of Yb impurities in Au in the presence of small (≤ 1 kG) external magnetic fields at 1.4 and 4.2 K. In this case dramatic changes occur in the hf spectra since the Zeeman and hf splittings are of the same order of magnitude. However, the relaxation rates are found to be independent of the field applied since the Zeeman and hf splittings (≤ 300 mK) are always small compared to the temperature of investigation (≥ 1.4 K). Thus, the Korringa law is still valid.

In this study we extend the measurements on Yb impurities in Au to higher fields. In particular, we report ME measurements at 4.2 K in external magnetic fields between 10 and 55 kG and at 50 kG in the temperature range from 4.2 to 40 K. As will be discussed below, it is important to note that the experiments were carried out as source experiments.

When strong ($\gtrsim 10$ kG) external magnetic fields are applied several new phenomena arise. At first, the Zeeman energy will be comparable to the crystalline-electric-field (CEF) energy, leading to an admixing of the various CEF wave functions. For a cubic CEF the admixture of the anisotropic Γ_8 CEF state will result in a finite magnetic anisotropy of all $2J+1$ states belonging to the free-ion ground state. For Mössbauer studies on polycrystalline samples one then has to average over all external field directions with respect to the cubic axes. Secondly, the Zeeman splitting, e.g., of the lowest CEF level, will be of the order of the temperature of investigation. In this case the simple Korringa law for the relaxation rates is no longer valid, because the frequency dependence of the spectral density of the conduction-electron bath has to be taken into account.[8,9]

In the study of Yb impurities in Au some particular aspects are of interest when comparing measurements with and without external magnetic fields. As has been shown previously,[8,9] in the ME a fundamental difference exists between source and absorber experiments, due to slow relaxation rearrangement in the electronic shell of the Mössbauer source atom after the β decay. Thus in the particular case of Yb impurities in Au one might expect finite intensity contributions to the ME spectrum from the upper Zeeman level of the Γ_7 CEF ground doublet, even when the upper level is separated far enough from the ground level to have negligible thermal population. The new rearrangement ideas automatically lead to the question of how the $4f$–conduction-electron interaction should be described. While the usual vector exchange ($\sim \vec{J} \cdot \vec{s}$) allows relaxation transitions between states only if the selection rule $\Delta J_z = 0, \pm 1$ is satisfied, a general coupling of the type considered previously by Coqblin and Schrieffer[10] and Hirst[11] will allow transitions between any two states. Finally, the

Kondo problem[12,13] of Yb in Au needs to be discussed since it is well known that the Kondo effect may be quenched in sufficiently high magnetic fields.[14]

In order to analyze the experimental results a general microscopic relaxation theory has been used which includes a general description of the $4f$-conduction-electron coupling and the possibility of frequency-dependent relaxation processes. This relaxation theory is written for a general nuclear transition, except for the special case of a diagonal hf interaction, which besides describing the present experiments is frequently encountered in Mössbauer spectroscopy.

II. THEORETICAL ASPECTS

A. Electronic Stark and Zeeman splitting

In the discussion of the electronic properties of the Mössbauer RE ion we will restrict ourselves to the discussion of the $[SL]$-J free-ion ground state, since excited $[SL]$-J states are typically a few thousand degrees Kelvin higher. For Yb^{3+} the Hund's ground state is $^2F_{7/2}$, which in presence of a cubic crystalline electric field (Stark effect) splits into two isotropic Kramers doublets Γ_6 and Γ_7 and a magnetically anisotropic Γ_8 quartet.[15] From susceptibility,[16,17] EPR,[18] and previous ME data[3,7] the Γ_7 doublet is known to be the CEF ground state for dilute Yb impurities in the fcc Au metal. According to Williams and Hirst[16] the excited states Γ_8 and Γ_6 are situated at 80 and 83 K, respectively. Independent measurements of Murani[17] essentially verify this result, although the separations are found to be slightly larger, i.e., 91 K (Γ_6) and 94 K (Γ_8).

An applied external magnetic field will in general lift the degeneracy of the Kramers states. In a previous paper[7] the case of weak ($\lesssim 1$ kG) external magnetic fields was discussed. In this case the separations between the CEF levels are larger than the Zeeman splittings (which are of the order of the hf splittings). Consequently, one could discuss the Zeeman effect separately for each CEF level.

In the presence of strong external magnetic fields ($H \gtrsim 10$ kG) the Zeeman splittings are comparable in magnitude to the CEF Stark splittings. Hence the Zeeman effect can no longer be treated by perturbation but rather one has to diagonalize the CEF and Zeeman Hamiltonians simultaneously. Using the CEF Hamiltonian for cubic symmetry in the notation of Lea, Leask, and Wolf[15] (LLW) (z axis along one of the fourfold axes) one obtains

$$\mathcal{H} = W\left(\frac{x}{F(4)}\,(O_4^0 + 5O_4^4) + \frac{1-|x|}{F(6)}\,(O_6^0 - 21O_6^4)\right) + g_J \mu_B (\vec{J}\cdot\vec{H}). \tag{1}$$

Here x and W are the CEF parameters in the LLW Hamiltonian, $F(4)$ and $F(6)$ are constants for a given J level, and the matrix elements of the operators O_n^m are given by Hutchings.[19]

Equation (1) can now be diagonalized for a given orientation of $\vec{H}$ with respect to the fourfold axes. As a solution one obtains $2J+1$ energies E_i and wave functions

$$\psi_i = \sum_{J_z} a_{J_z}^i \,|\, J, J_z\rangle\,. \tag{2}$$

The wave functions ψ_i will in general be a linear combination of the pure CEF wave functions, which, in the case of Yb^{3+}, are independent of the CEF parameters.[15] The degree of admixture of the CEF wave functions by the external magnetic field is in first order inversely proportional to the respective energy separation of the CEF states. In Sec. II B the wave functions ψ_i will be used to calculate the ME hf spectrum.

B. Static ME spectrum

The magnetic part of the ME spectrum is given by the eigenvalues of the Hamiltonian[20]

$$\mathcal{H}_M = A(\vec{J}\cdot\vec{I}), \tag{3}$$

where the wave functions ψ_i are used for diagonalization. Since the CEF and Zeeman energies E_i are much larger than the hf energies, the hf interaction can be regarded separately for the $2J+1$ electronic states ψ_i. The hf matrix elements are given by

$$A \sum_{j=x,y,z} \langle \psi_i | \hat{J}_j | \psi_i \rangle \langle I_z | \hat{I}_j | I_z' \rangle\,. \tag{4}$$

For an arbitrary orientation of the external magnetic field with respect to the cubic axes the off-diagonal matrix elements in Eq. (4) (e.g., $\langle \psi_i | \hat{J}_+ | \psi_i \rangle$) will not vanish in general. This is due to a finite anisotropy of all states ψ_i caused by an admixing of the CEF wavefunctions by the external magnetic field. In the specific case of Yb impurities in Au the ME spectrum is basically determined by the two lowest electronic states, i.e., the Zeeman levels of the originally isotropic Γ_7 CEF ground doublet (compare Fig. 1). Because of the large energy separation from the Γ_8 quartet (Γ_6 and Γ_7 cannot mix directly) the anisotropy of the lowest two states is expected to be quite small. Thus, Eq. (4) will in good approximation take the diagonal "effective-field" form

$$\mathcal{H}_M = A\langle \psi_i | \hat{J}_z | \psi_i \rangle I_z = -H_{\mathrm{eff}} g_N \mu_N I_z\,. \tag{5}$$

In Eq. (5) only the contribution of the $4f$ shell to the ME spectrum has formally been considered. However, other contributions to the effective field at the nucleus, e.g., from polarization of the conduction electrons by the $4f$ moment, are absorbed

in the hf coupling constant A, which has been derived for Yb impurities in Au by EPR[18] and ME[7] measurements and found to be 4.55 mm/sec (1.28×10^{-6} eV) for the ^{170}Yb isotope. When compared to the value $A = 4.40$ mm/sec derived for insulator hosts,[18] one finds that there is indeed a small contribution to the hf field from conduction-electron polarization by the $4f$ moment.[18,21] Even a larger contribution of this kind has been observed for Er impurities in Th.[5] It should be noted that for RE elements the direct contribution from applied magnetic fields is negligible compared to the $4f$ hf field $H_{4f} \approx H_{\text{eff}} \approx 3$ MOe.

In addition to the magnetic hf interaction, in the presence of magnetic fields there will be a quadrupole hf interaction. Although the cubic environment of the Au lattice does not contribute to the quadrupole interaction, the $4f$ shell will in general produce an electric field gradient (EFG). Even without application of an external magnetic field a quadrupole interaction may arise from the anisotropic Γ_8 state,[4] while the quadrupole interaction is zero for both doublets, Γ_6 and Γ_7. In the presence of external magnetic fields each of the $2J+1$ electronic energy states will produce an EFG. While even isolated Kramers states in the presence of a strong Zeeman field (which lowers the symmetry) will in general support electric quadrupole fields, an EFG also arises from an admixing of different CEF states. In a frame of reference with the z axis along the direction of the external magnetic field the quadrupole coupling is given by[20]

$$\mathcal{H}_Q = B \langle \psi_i | 3\hat{J}_z^2 - J(J+1) | \psi_i \rangle [3I_z^2 - I(I+1)], \quad (6)$$

where B is defined as[20]

$$B = -e^2 Q \langle J \| \alpha \| J \rangle \langle r^{-3} \rangle / 4I(2I-1) . \quad (7)$$

For Yb^{3+} the free-ion value may be calculated as $B(^{170}\text{Yb}) = 0.125$ mm/sec (3.5×10^{-8} eV). While the atomic Sternheimer shielding is small for Yb^{3+},[22] estimates of conduction-electron contributions to B in cubic hosts are difficult at present. We will, therefore, use the above value for B in the analysis of our results.

For a given orientation of $\vec{H}$ with respect to the four-fold axes, the ME spectrum is given by the eigenvalues of

$$\mathcal{H}_{\text{hf}} = \mathcal{H}_M + \mathcal{H}_Q . \quad (8)$$

From Eq. (8) we have omitted a term for an isomer shift, since it is very small for ^{170}Yb and may be neglected for our purposes. The total ME spectrum for a polycrystalline sample is obtained by averaging the line positions which follow from Eq. (8) over all directions of the external magnetic field. The averaging may be approximated as follows[23]: Eq. (1) is solved for $\vec{H} \| [001]$, $\vec{H} \| [111]$, and $\vec{H} \| [110]$, where the CEF Hamiltonians for the three respective directions (H defines the z axis) are derived by Hutchings.[19] The Mössbauer spectra $I(001)$, $I(111)$, and $I(110)$ are then calculated with the respective wave functions ψ_i and averaged

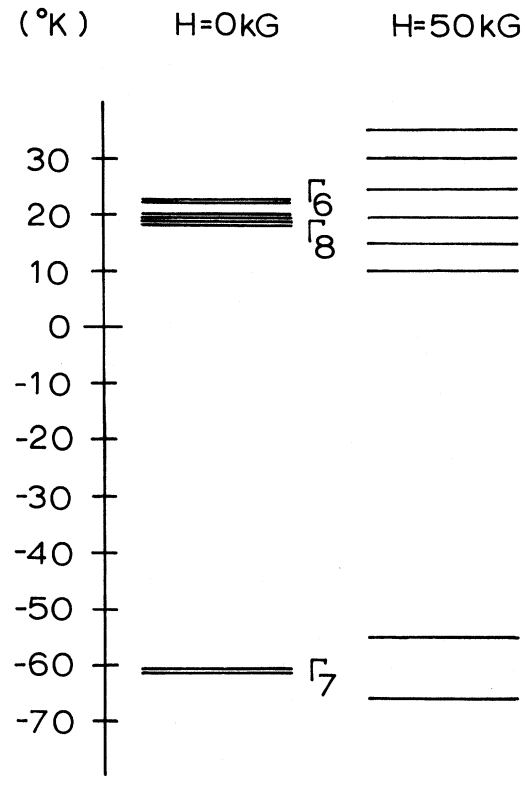

FIG. 1. Electronic energy levels of the $^2F_{7/2}$ free-ion ground state of Yb^{3+} in the presence of the cubic crystalline electric field of the Au host ($H = 0$ kG) and an additional applied external magnetic field ($H = 50$ kG), assuming $x = 0.77$ and $W = 3.65$ K.

TABLE I. Orientational dependence of Zeeman splitting (E_i), magnetic moments ($S_i = \langle \psi_i | \hat{J}_z | \psi_i \rangle$), and field gradients [$Q_i = \langle \psi_i | 3\hat{J}_z^2 - J(J+1) | \psi_i \rangle$] for the ground ($i = 1$) and first excited ($i = 2$) electronic states at 55 kG. CEF parameters $x = 0.77$ and $W = 3.65$ K were used.

	Axes		
	Twofold [110]	Threefold [111]	Fourfold [001]
E_2	12.61	12.64	12.53
E_1	0	0	0
S_2	1.16	1.17	1.13
S_1	−1.80	−1.81	−1.77
Q_2	−1.99	−2.28	−1.11
Q_1	2.24	2.71	0.81

according to[23]

$$I_{\text{tot}} = \tfrac{1}{26}[6I(001) + 8I(111) + 12I(110)]\,. \tag{9}$$

In Table I we have listed values for E_i, $S_i = \langle\psi_i | \hat{J}_z | \psi_i\rangle$, and $Q_i = \langle\psi_i | 3\hat{J}_z^2 - J(J+1) | \psi_i\rangle$ for the lowest two energy levels ($i = 1, 2$) as calculated for the three external field directions [001], [111], and [110] and for $H = 55$ kG and the CEF parameters $x = 0.77$ and $W = 3.65$ K taken from Ref. 16. As expected, the Zeeman splitting (E_i) and the magnetic moments ($\sim S_i$) are nearly independent of orientation, indicating that the magnetic anisotropy of the lowest two states in the presence of magnetic fields up to 55 kG is small. However, the EFGs ($\sim Q_i$) show an orientational dependence. In this case the simplified averaging over all directions by means of Eq. (9) is acceptable only because the quadrupole interaction is small as compared to the magnetic hf interaction.

The Mössbauer line positions as calculated from Eq. (8), however, only describe the experimental ME spectrum in the limit of long electronic relaxation times, i.e., when the electronic relaxation time t_R is much longer than the nuclear correlation time $t_{\text{hf}} = (\omega_{\text{hf}})^{-1}$, where ω_{hf} is the hf splitting. For Yb, $\omega_{\text{hf}} = 15$ mm/sec (Ref. 24), leading to $t_{\text{hf}} \approx 2\times10^{-10}$ sec. In our previous study of dilute Au:Yb alloys in the absence of any external magnetic field or in weak magnetic fields we have derived a relaxation rate of $R = 452$ MHz at 4.2 K.[7] This yields a relaxation time of $t_R = 1/2\pi R \approx 3\times10^{-10}$ sec. In the system under investigation one is thus in the region $t_R \approx t_{\text{hf}}$, which for the study of relaxation effects is the most interesting one. On the other hand, our estimates indicate that the description of the ME spectrum in the static limit given above will not be sufficient to describe the experimental ME spectra, but rather relaxation processes have to be taken into account.

At the temperatures considered in this study ($T \leq 40$ K) it seems likely that the relaxation effects in the Mössbauer spectrum will result mainly from the coupling of the $4f$ electronic shell to the conduction electrons. The relaxation contributions due to phonons are expected to be relatively small, and the following discussion will be made upon the assumption that they can be neglected.

C: $4f$-conduction-electron coupling

The coupling of the $4f$ shell to the conduction-electron bath results in temperature-dependent spin flip or relaxation processes among the electronic energy levels. These dynamical effects in the electronic shell manifest themselves in the Mössbauer spectrum through the hf interaction. Since the direct coupling of the nucleus to the conduction-electron bath is much smaller than both the hf interaction and the $4f$–conduction-electron interaction, it is usually neglected for the calculation of the relaxation ME spectrum.

In the study of relaxation processes in the electronic shell by means of Mössbauer-source experiments the description of the $4f$–conduction-electron coupling plays an important role. In order to describe and physically understand the relaxation rearrangement in the electronic shell following the nuclear β decay a realistic description of the impurity–conduction-electron interaction is needed. Since we are interested in relaxation processes among the levels belonging to the electronic ground configuration of the Mössbauer atom, a configuration-based or Schrieffer-Wolff[25] approach is adequate.[26] In such a model the inner-atomic interactions of the impurity plus the CEF interaction are treated in detail, while the Anderson mixing interaction[27] between the impurity electrons and the conduction electrons is treated as a perturbation.[26]

In order to describe the general interaction of a localized $4f$ or $3d$ spin with the conduction electrons it is advantageous to make use of the irreducible-tensor method. As was first shown by Hirst,[11] this group-theoretical method may be related to the general types of k-f or k-d coupling that are yielded by the realistic microscopic theories.[26] For a metal such as Au, in which electrons at the Fermi surface can be treated as free electrons,[28] it is appropriate to describe the k-f or k-d interaction initially in terms of free-electron partial-wave conduction-electron states $|k, l, m, \sigma\rangle$. The impurity states are taken initially as the states $|L, M_L, S, M_S\rangle$ belonging to the L-S ground term. Within this framework the most general possible interaction can be written[11]

$$\mathcal{H}_I = \sum_{\substack{kl\Lambda\Sigma \\ k'l'\mu\nu}} I_{LS}{}^{l'l\Lambda\Sigma}\,(B_{LS}{}^{\Lambda\Sigma}_{\mu\nu})^{\dagger} C_{LS}{}^{k'l'kl}{}^{\Lambda\Sigma}_{\mu\nu}\,, \tag{10}$$

where I_{LS} is a coupling constant, B_{LS} is a tensor operator acting on the impurity, and C_{LS} is a tensor operator acting on the conduction electrons. The operators B_{LS} and C_{LS} are unit spherical double-tensor operators, which are defined so as to have a natural normalization and simple behavior under rotational transformations.[11] Rewriting Eq. (10) as

$$\mathcal{H}_I = \sum_{\substack{\Lambda\Sigma \\ \mu\nu}} (B_{LS}{}^{\Lambda\Sigma}_{\mu\nu})^{\dagger} F_{LS}{}^{\Lambda\Sigma}_{\mu\nu}\,, \tag{11}$$

the spectral density of the conduction-electron bath is given by the Fourier transform of the autocorrelation function

$$\langle\langle F_{LS\,\mu\nu}^{\Lambda\Sigma}(t)[F_{LS\,\mu'\nu'}^{\Lambda'\Sigma'}(t-\tau)]^{\dagger}\rangle\rangle = \delta_{\Lambda\Lambda'}\,\delta_{\mu\mu'}\,\delta_{\Sigma\Sigma'}\,\delta_{\nu\nu'}\,G_{LS}^{\Lambda\Sigma}(\tau, T)\,. \tag{12}$$

The spectral density, which, as will be discussed below, is closely connected with the relaxation processes in the impurity, is then given by[29]

$$J_{LS}^{\Lambda\Sigma}(\omega, T) = \int_{-\infty}^{\infty} d\tau\, e^{-i\omega\tau}\, G_{LS}^{\Lambda\Sigma}(\tau, T) = 2\pi \sum_{ll'} |I_{LS}^{l'l\Lambda\Sigma}\,\rho_U^1(E_F)|^2\, \frac{\omega}{e^{\omega/kT}-1}\,. \tag{13}$$

Here $\rho_U^1(E_F)$ is the conduction-electron density of states at the Fermi surface per spin direction.[29]

The above considerations are valid for $4f$ as well as $3d$ impurities. In the following we will consider a generalized Schrieffer-Wolff coupling[25,26] which corresponds to a specialization of Eq. (10) with $l=l'=3$ for $4f$ and $l=l'=2$ for $3d$ impurities. Furthermore, we will restrict our discussion to the case of Yb^{3+}, which is particularly simple since its configuration $4f^{13}$ corresponds to a single $4f$ hole in the full $4f$ shell. It should be noted, however, that the tensor method is readily capable of treating any number of $4f$ or $3d$ electrons, as will be shown by L. L. Hirst in a separate paper.[30] In the case of Yb^{3+} the coupling constant is simply $I_{LS}^{l'l\Lambda\Sigma} = I_C\,\delta_{l,3}\,\delta_{l',3}$, independent of Λ and Σ. Here

$$I_C = |V_{kf}|^2\,(1/E_{\rm exc}^{(+)} + 1/E_{\rm exc}^{(-)})\,, \tag{14}$$

where V_{kf} is the mixing interaction strength and $E_{\rm exc}^{(\pm)}$ is the energy necessary to make an interconfigurational excitation from $4f^N$ to $4f^{N\pm1}$. With this coupling, the spectral density of Eq. (13) takes the form

$$J_{LS}^{\Lambda\Sigma}(\omega, T) = J_{LS}(\omega, T) = 2\pi |I_C\,\rho(E_F)|^2\, \frac{\omega}{e^{\omega/kT}-1}\,, \tag{15}$$

where we have defined $\rho(E_F) = \rho_U^1(E_F)$. The dimensionless expression $|I_C\rho(E_F)|^2$, which symbolizes a coupling strength, will in practice be treated as a fitting parameter.

Since we want to treat relaxation processes only between the lowest electronic energy states, i.e., between the $2J+1$ energy states ψ_i given by Eq. (2), the tensor operators given by Eqs. (10) or (11) need to be projected onto the Hund's free-ion ground state. While the detailed mathematical treatment will be published elsewhere,[30] let us here only state the result. Projection onto the $[SL]$-J ground state yields

$$\mathcal{H}_I = \sum_{\substack{1\le Q\le 7\\ -Q\le q\le Q}} (B_q^Q)^{\dagger}\, F_q^Q = \sum_{Q,q} B_q^Q\,(F_q^Q)^{\dagger}\,. \tag{16}$$

Here, the spherical tensor operators B_q^Q and F_q^Q describe the impurity and bath, respectively, and for RE ions only tensor operators with $Q \le 7$ are defined. Matrix elements of the operators B_q^Q are given by

$$\langle J, J_z'|\,B_q^Q\,|J, J_z\rangle = (-1)^{J-J_z'}(2Q+1)^{1/2}\begin{pmatrix} J & Q & J \\ -J_z' & q & J_z\end{pmatrix}, \tag{17}$$

where the last bracket in Eq. (17) is a 3-j symbol.[31] The new spectral density complimentary to B_q^Q is given by

$$J^Q(\omega, T) = \int_{-\infty}^{\infty} d\tau\, e^{-i\omega\tau}\ \langle\langle F_q^Q(t)\,[F_{q'}^{Q'}(t-\tau)]^{\dagger}\rangle\rangle\,. \tag{18}$$

If the tensor operators F_q^Q are expressed in terms of the tensor operators F_{LS} of Eq. (11), the spectral density $J^Q(\omega, T)$ can be found in terms of $J_{LS}(\omega, T)$. In the case of Yb^{3+}, this spectral density takes a particularly simple, Q-independent form, namely,

$$J^Q(\omega, T) = J(\omega, T) = 2\pi\,|I_C\,\rho(E_F)|^2\,\omega/(e^{\omega/kT}-1). \tag{19}$$

The spectral density summarizes all the information about relaxation forces in the conduction-electron bath which is relevant to the calculation of relaxation processes in second-order perturbation theory. In particular, the rate $R_{i\to j}$ at which a transition from an impurity state i to a state j is driven by the bath is just proportional to [see Eq. (35) below]

$$R_{i\to j} \sim J(\omega_{ji}, T) = 2\pi\,|I_C\,\rho(E_F)|^2\,\omega_{ji}/(e^{\omega_{ji}/kT}-1), \tag{20}$$

where $\omega_{ji} = E_j - E_i$. The spectral density satisfies the important identity $J^Q(-\omega, T) = e^{\omega/kT}\,J^Q(\omega, T)$, which states that a transition from a higher to a lower level proceeds more rapidly than the transition in the reverse direction. Consequently, the bath always tends to drive the populations of the impurity levels toward their thermal-equilibrium values.

Finally, the generalized k-f tensor coupling should be compared to the simple case of a vector exchange

$$H_{\rm ex} = \sum_{k'k\sigma'\sigma} -2(g_J-1)J_{sf}\,\vec{\mathbf{J}}\cdot\vec{\mathbf{s}}_{\sigma'\sigma}\,c_{k'00\sigma'}^{\dagger}\,c_{k00\sigma}\,, \tag{21}$$

where g_J is the Landé factor and $c_{k00\sigma}$ is an annihilator for a conduction-electron state in the $l=0$ partial wave. The coupling (21) is equivalent to a special case of the tensor coupling, Eq. (16), in which the contributions for $Q\neq1$ vanish. Specifically,[31]

$$J_z = [P(J)]^{1/2}B_0^1\,,\quad J_{\pm}/\sqrt{2} = \mp[P(J)]^{1/2}B_{\pm1}^1\,, \tag{22}$$

where $P(J) = \frac{1}{3}(2J+1)(J+1)J$. Similarly, the combination $\vec{\mathbf{s}}\,c^{\dagger}$ c appearing in Eq. (21) is proportional to the corresponding components of the tensor

operator C_{LS} with proportionality factor $[P(s)]^{1/2}$. The spectral density produced by Eq. (21) is given by Eq. (20) with

$$|I_c\rho(E_F)|^2 = 4P(J)\,P(s)\,|(g_J-1)\,J_{sf}\rho(E_F)|^2 \ . \qquad (23)$$

In the past, the exchange coupling (21) has always been applied to the description of Mössbauer relaxation phenomena. However, as noted above, an interaction of the generalized Schrieffer-Wolff type, containing a sum of all possible types of tensor couplings, is to be expected from a realistic microscopic point of view. We shall use such an interaction in our discussion of relaxation effects. As will be discussed below, it turns out that this more general coupling form is indeed necessary to describe the relaxation phenomena in Mössbauer-source experiments.

D. Population of electronic energy levels after β decay

It has been pointed out previously[8,9] that relaxation phenomena in Mössbauer-source experiments are intimately connected with the process of electronic rearrangement which takes place in response to the nuclear transformation. These electronic-rearrangement processes have been completely neglected in the past, as from an oversimplified point of view they were considered to be too fast to be seen in a ME experiment. Since the understanding of the rearrangement processes is essential for the understanding and the calculation of the ME relaxation spectra, we will briefly outline the basic ideas below.

The radioactive β decay of ^{170}Tm(130d), which directly feeds the $2^+ \rightarrow 0^+$ 84.3-keV Mössbauer transition of ^{170}Yb, starts both the Mössbauer γ emission, and the rearrangement in the electronic shell in response to the change in nuclear charge. The first step of rearrangement in the electronic shell is a change in configuration, i.e., from $4f^{12}(\mathrm{Tm}^{3+})$ to $4f^{13}(\mathrm{Yb}^{3+})$. In order to compensate for the increase in nuclear charge a conduction electron is absorbed into the $4f$ shell by means of the Anderson mixing interaction.[27] The rate R for this process may be estimated by application of the "Golden Rule," viz., $\hbar R = \Delta = \pi |V_{kf}|^2 \rho(\epsilon)$.[32] Assuming a virtual bound state width $\Delta \approx 0.01$ eV for Yb^{3+}, the time for the change in configuration is estimated to be $\hbar/\Delta \approx 10^{-13}$–$10^{-14}$ sec. When compared to the nuclear lifetime $t_N \approx 10^{-9}$ sec, the interconfigurational rearrangement is indeed fast.

The decay of the configuration $4f^{12}$ into $4f^{13}$ leaves the ground configuration in a highly excited state. Rearrangement within $4f^{13}$ will then proceed via energy exchange with the conduction-electron bath. The transition rates $R_{i\rightarrow j}$ between any two states i and j within $4f^{13}$ are proportional to the spectral density given by Eq. (20), where the proportionality factors (matrix elements) which depend upon the specific transition of interest are of the order of unity. For a transition from a state i to a lower state j separated by $\omega_{ij} \gg kT$ it is seen from Eq. (20) that because ω_{ji} is negative the decay rate will be equal to $2\pi|\omega_{ji}||I_c\rho(E_F)|^2$. Only those electronic states will then contribute to the ME spectrum which decay in a time comparable to the nuclear lifetime. It is important to note that the *intensity* of the hf structure of a given electronic level depends on the comparison of its decay time to the nuclear lifetime ($t_N \approx 10^{-9}$ sec for ^{170}Yb) while the detailed *shape* of the respective hf spectrum depends on the relation between the decay time and the nuclear correlation time ($t_{\mathrm{hf}} \approx 10^{-10}$ sec for ^{170}Yb).

In the case of Yb^{3+} there is only one excited $[SL]$-J state above the free-ion ground state $^2F_{7/2}$, namely, $^2F_{5/2}$ at approximately 15 000 K. Thus a simple estimate indicates that the decay of the electronic shell into the $^2F_{7/2}$ ground state is quasi-instantaneous. However, rearrangement or what is equivalent, relaxation processes between the CEF or Zeeman levels of the $^2F_{7/2}$ ground manifold, are not necessarily fast on the Mössbauer time scale. In particular, electronic levels which lie in the range of 1–10 K above the ground level[33] will decay with times comparable to the nuclear lifetime.

For treating Mössbauer-relaxation phenomena it is necessary to know the *initial* population of the electronic-nuclear system. In the case of the ME, "initial" means at the beginning of γ-ray emission or absorption. Since our above estimates indicate that the change of the electronic shell into its $^2F_{7/2}$ ground state is quasi-instantaneous on the Mössbauer time scale, the initial population of the electronic shell in a *source* experiment can be represented quite accurately by an equal population of all states within $^2F_{7/2}$. This is in contrast to the *absorber* case where a Boltzmann initial population is assumed. Unfortunately at present no quantitative solution for Mössbauer source spectra with electronic rearrangement effects exist. The respective equations of motion have only been solved for the case of an absorber experiment.[34] In Sec. II E we shall consider these equations of motion and the resulting Mössbauer relaxation spectrum by allowing for a generalized-tensor-type $4f$ conduction-electron coupling and frequency dependent relaxation processes between the electronic energy levels. Within this formalism we shall somewhat account for rearrangement by assuming an equal initial population of all levels within $^2F_{7/2}$.

E. ME spectrum in the presence of relaxation effects

In the calculation of the ME spectrum we will essentially follow the microscopic theory of Hirst.[34] Let us consider a Mössbauer transition between a hf state $|a\rangle$ belonging to the excited nuclear state and a hf state $|d\rangle$ of the nuclear ground state, described by a transition operator M. Then the Mössbauer spectrum is given by the real part of the Fourier transform of the correlation function $G(t) = \ll [M(0)]^\dagger M(t) \gg$,[35] namely,

$$I(\omega) = \int_0^\infty dt\, e^{-i\omega t} G(t) \ . \tag{24}$$

The calculation of the ME spectrum given by Eq. (24) then consists in solving the equation of motion for the matrix elements $M_{ad}(t)$. Writing the coupling between the $4f$ and conduction electrons in the form of Eq. (16), the equation of motion is given by[36]

$$\frac{d}{dt} M_{ad}(t) = (i\omega_{ad} - \tfrac{1}{2}\Gamma_{\min}) M_{ad}(t) + \tfrac{1}{2}\Bigg(\sum_{Q,a,b,c} - (B_q^Q)^\dagger_{ab} (B_q^Q)_{bc} M_{cd}(t)\, J^Q(\omega_{bc}, T) + (B_q^Q)^\dagger_{ab} M_{bc}(t) (B_q^Q)_{cd}\, J^Q(\omega_{cd}, T)$$
$$+ (B_q^Q)^\dagger_{ab} M_{bc}(t) (B_q^Q)_{cd}\, J^Q(\omega_{ba}, T) - M_{ab}(t) (B_q^Q)^\dagger_{bc} (B_q^Q)_{cd}\, J^Q(\omega_{cb}, T) \Bigg) . \tag{25}$$

The spectral density $J^Q(\omega, T)$ is given by Eq. (20) and $\Gamma_{\min}$ is the minimum experimental line width (full width at half maximum, FWHM). A pair of bra and ket indices may be combined into a single state pair index, e.g., $M_{ad}(t) \to M_k(t)$. The index k then distinguishes the allowed Mössbauer transitions. With $\vec{M}(t)$ as a column vector, Eq. (25) becomes the matrix equation

$$(d/dt)\vec{M}(t) = (i\underline{\omega}' + \underline{R})\vec{M}(t) \ , \tag{26}$$

where $(\underline{\omega}')_{kl} = (\omega_k + \frac{1}{2} i\Gamma_{\min})\delta_{kl}$ and $\underline{R}$ is the relaxation matrix defined by Eq. (25). From the indices of the relaxation-matrix elements (e.g., $R_{kl} = R_{ad\ bc}$) an important feature of the relaxation processes is evident. Relaxation in the Mössbauer effect must be understood not as spin flips between the hf eigenstates but rather as a switching between the possible Mössbauer γ transitions (e.g., from $a \to d$ to $b \to c$). The solution of Eq. (26) is given by

$$\vec{M}(t) = [\exp(i\underline{\omega}' + \underline{R})t]\vec{M}(0) \ . \tag{27}$$

With $G(t) = [\vec{M}(0)]^\dagger \underline{W} M(t)$, where $\underline{W}$ is the diagonal density matrix describing the initial preparation of the Mössbauer atom, the relaxation Mössbauer spectrum is obtained as[37]

$$I(\omega) = \mathrm{Re}\{[\vec{M}(0)]^\dagger \underline{W}(i\omega\underline{E} - i\underline{\omega}' - \underline{R})^{-1}\vec{M}(0)\} \ , \tag{28}$$

where $\underline{E}$ is the unit matrix.

For $\underline{R} = 0$ the Mössbauer spectrum is given by the familiar Lorentz-line-shape formula

$$I(\omega) \sim \mathrm{Re}\sum_k \left(\frac{1}{i(\omega - \omega_k) + \frac{1}{2}\Gamma_{\min}} \right) \ . \tag{29}$$

The ω_k are the static-limit Mössbauer line positions, e.g., the eigenvalues of Eq. (8). In the presence of relaxation, the evaluation of Eq. (28) is in general nontrivial, since the relaxation matrix may be of large dimensionality. As was pointed out by Wickman,[38] the solution of Eq. (28) is simplified if the hf interaction is diagonal. In the following we will also consider this case since it describes the experimental situation of *Au*:Yb in strong external magnetic fields.

Since M acts as a transition operator, the matrix elements $M_{ad} = \langle a | T_k^q | d \rangle$ may be evaluated by means of the Wigner-Eckart theorem.[31] In the case of a diagonal hf interaction and a nuclear transition between the excited Mössbauer state I and the ground state I' the hf states $|a\rangle$ and $|d\rangle$ will be pure in the nuclear spin, and one thus obtains

$$M_{ad} = \langle a | T_k^q | d \rangle$$
$$= \langle I', I_z', k, q | I, I_z \rangle F_k^q(\Theta) \langle I' \| T_k \| I \rangle \ , \tag{30}$$

where the quantities on the right side of Eq. (30) are the Clebsch-Gordan (CG) coefficients, the polarization factors,[39] and a reduced matrix element. While the reduced matrix element is just a constant and the polarization factors average to a constant value for a polycrystalline sample, the CG coefficients have to be calculated for the various transitions. However, in the case of the pure $E2$ $2 \to 0$ transition in ^{170}Yb all five CG coefficients are equal. Furthermore, since only the relative intensities of the possible Mössbauer lines are of interest we can normalize $M_{ad} = 1$. Thus the row and column vectors $[M(0)]^\dagger$ and $\vec{M}(0)$ in Eq. (28) are unit vectors in the case of ^{170}Yb. While the above considerations for the relative ME intensities are sufficient for absorber experiments, for source experiments the radiative feeding of the hf states of the excited Mössbauer state needs to be considered. In the system under investigation the 1^- nuclear ground state of ^{170}Tm provides the radioactive feeding of the 2^+ excited Mössbauer state of ^{170}Yb.[40] Tm in Au has a Γ_2

nonmagnetic CEF ground state with the next higher magnetic state being a Γ_5 triplet at approximately 7 K.[16] Even in the presence of external magnetic fields ($\lesssim 50$ kG) the electronic-magnetic moment at 4.2 K will be considerably less than the free-ion moment and hence the splitting of the 1^- nuclear ground state of ^{170}Tm is not likely to exceed 100 mK. Since our investigations were carried out at 4.2 K, an equal radioactive feeding of the excited hf states in ^{170}Yb can be assumed and thus $M_{ad}=1$ will be a good assumption.

Next, the density matrix $\underline{W}$ needs to be considered. For a diagonal hf interaction only the initial population of the electronic energy states is important, since relaxation processes do not exist between the nuclear states. As has been shown in an earlier section of this paper the electronic-density matrix is simply a diagonal unit matrix in the case of source experiments and a diagonal matrix with Boltzmann factors as diagonal elements in the case of absorber experiments.

The diagonal matrices $\omega\underline{E}$ and $(\underline{\omega}')_{kl}=(\omega_k+\frac{1}{2}i\Gamma_{\min})\delta_{kl}$ contain the velocity points ω of the Mössbauer spectrum, the static-limit Mössbauer-line positions ω_k [eigenvalues of Eq. (8)], and the static-limit width $\Gamma_{\min}$. In the case of ^{170}Yb the matrices are of dimensionality $(2J+1)\times(2I+1)=40$, but the dimensionality can be reduced to 8, as will be discussed below.

The calculation of the relaxation matrix is considerably easier in the effective-field case than in the general case. Let us consider a spin-flip process from an electronic state ψ_i to another state ψ_j $(i\neq j)$, described by a matrix element $R_{ij}=R_{ad\,bc}$. From Eq. (25) we obtain

$$R_{ij}=R_{ad\,bc}=\frac{1}{2}\sum_{Q,q}[(B_q^Q)^\dagger_{ab}(B_q^Q)_{cd}J^Q(\omega_{cd},T)+(B_q^Q)^\dagger_{ab}(B_q^Q)_{cd}J^Q(\omega_{ba},T)]\ . \quad (31)$$

Since the hf eigenvectors $|a\rangle$, $|b\rangle$, $|c\rangle$, and $|d\rangle$ are pure in the nuclear quantum numbers and the operators B_q^Q only act on the electronic quantum numbers, the states $|a\rangle$ and $|b\rangle$, on one hand, and $|c\rangle$ and $|d\rangle$, on the other hand, have to agree in nuclear quantum numbers. Furthermore, the excited and ground states of an allowed Mössbauer transition always see the same effective field (i.e., the same ψ_i). Accordingly, for a Mössbauer transition from I to I', the hf states have the structure

$$|a\rangle=|\psi_i,I,I_z\rangle\ ,\quad |b\rangle=|\psi_j,I,I_z\rangle\ ,\quad |d\rangle=|\psi_i,I',I_z'\rangle\ ,\quad |c\rangle=|\psi_j,I',I_z'\rangle\ . \quad (32)$$

The off-diagonal relaxation-matrix elements are

$$R_{ij}=R_{ad\,bc}=\sum_{Q,q}|\langle\psi_j|B_q^Q|\psi_i\rangle|^2J^Q(\omega_{ji},T)\ . \quad (33)$$

Similarly, the diagonal relaxation-matrix elements are found to be

$$R_{ii}=-\sum_j R_{ij}\ . \quad (34)$$

With the wave functions given by Eq. (2), the matrix elements of Eq. (17), and the spectral density of Eq. (20), the relaxation matrix for Yb is given by

$$R_{ij}=2\pi|I_c\rho(E_F)|^2\frac{\omega_{ji}}{e^{\omega_{ji}/kT}-1}\times\sum_{\substack{1\le Q\le 7\\ -Q\le q\le Q}}\sum_{J_z,J_z'}(2Q+1)\left[a^i_{J_z}\,a^j_{J_z'}\begin{pmatrix}J & Q & J\\ -J_z' & q & J_z\end{pmatrix}\right]^2\ . \quad (35)$$

As is evident from both the relaxation matrix in Eq. (33) and the hf eigenvectors in Eq. (32), a spin flip from ψ_i to ψ_j corresponds to a change of the Mössbauer transition $a\to d$ to the transition $b\to c$. Furthermore the nuclear-spin quantum numbers do not change during a spin flip. Consequently, the total relaxation matrix in Eq. (28) has block diagonal form, where each submatrix is given by Eq. (35) and corresponds to the $2J+1$ nuclear transitions which have the same nuclear quantum numbers. Equation (28) can be written

$$I(\omega)=\sum_n \mathrm{Re}[(\vec{\epsilon}_n)^\dagger\underline{W}(\underline{\alpha}_n-\underline{R})^{-1}\vec{\epsilon}_n]\ , \quad (36)$$

where $(\vec{\epsilon}_n)^\dagger$ and $\vec{\epsilon}_n$ are $(2J+1)$-dimensional unit row and column vectors in case of a $2\to 0$ nuclear transition.[41] $\underline{W}$ is the unit matrix for source experiments, and a diagonal matrix with Boltzmann factors as diagonal elements in the case of an absorber experiment. The diagonal matrix $(\underline{\alpha}_n)_{ij}=[i(\omega-\omega_j^n)+\frac{1}{2}\Gamma_{\min}]\delta_{ij}$ contains the Mössbauer velocity points ω, the static-limit width [full width at half-maximum (FWHM)] $\Gamma_{\min}$, and the static-limit Mössbauer-line positions ω_j^n. The index n denotes a given set of nuclear quantum numbers (e.g., ω_j^1 denotes the $2J+1$ transitions with $I_z=2\to I_z'=0$). The index j indicates which electronic state ψ_j produces the eigenvalue ω_j^n [compare Eqs. (5) and (6)]. The $(2J+1)$-dimensional relaxation matrix R_{ij} is given by Eqs. (35) and (34).

Relaxation effects for the effective-field ME spectrum have been considered by several authors.[42] Previous microscopic relaxation theories[43] were limited in their applicability since they were only written for relaxation processes within an electronic doublet and they assumed both a vector exchange as well as a non-frequency-dependent spectral density (Korringa law). As is seen from Eq. (35) the general theory presented above includes the previous microscopic theory[43] in case of an effective-field hf interaction. For

an electronic doublet Eq. (35) is a 2×2 matrix, a vector exchange is described by $Q=1$, and for $kT \gg |\omega_{ji}|$ we obtain the Korringa law. On the other hand, from the stochastic theories[38,42] no insight into the nature of the $4f$–conduction-electron coupling can be obtained. For example, when Eq. (36) is compared to Wickman's expression for the relaxation Mössbauer spectrum [e.g., Eq. (29) in Ref. 38], both expressions can be shown to be equivalent if one defines $R_{ij}=-P_{ji}$. However, the relaxation matrix elements P_{ji} are not microscopically defined in Wickman's stochastic theory. Furthermore, all previous stochastic theories fail in the case of frequency-dependent relaxation processes. In fact, they might lead to an incorrect treatment of the frequency dependence, as for example in the case of Fe in Mo.[44]

III. EXPERIMENTAL

A. Mössbauer measurements

Alloys were prepared by induction melting of an appropriate quantity of radioactive ^{170}Tm ($T_{1/2}$ = 130 d) with Au (99.999% purity) in a graphite crucible under a purified argon atmosphere. The sample used in the present study contained 400 ppm of Tm. After pressing to a flat disc in order to reduce electronic absorption of the γ rays by the Au matrix and strain annealling for 4 h at 600 °C, the alloy was used as the source in a ME experiment. The decay of ^{170}Tm feeds the 84.3-keV ($2^+\rightarrow0^+$) Mössbauer resonance in ^{170}Yb. The resonance spectra of the source were analyzed with a "single-line" $YbAl_3$ (Ref. 45) absorber (65% enriched in ^{170}Yb) with a thickness of 20-mg ^{170}Yb per cm^2. The minimum experimental line width (FWHM) of this absorber was found to be $\Gamma_{min}=3.9\pm0.1$ mm/sec at 4.2 K with a single-line $TmAl_2$ source.

In the experiments both source and absorber were placed in a superconducting magnet with the magnetic field along the direction of γ-ray propagation. The superconducting coil produced magnetic fields up to $H=55$ kG. For the experimental arrangement described above and in the case of a $2\rightarrow0$ Mössbauer transition only the transitions corresponding to $\Delta I_z=\pm1$ are obtained because of γ-ray polarization.[39] In the *Au*:Tm source each of the electronic states ψ_i will in general produce a two-line ($\Delta I_z=\pm1$) hf spectrum, although the intensity contribution from the excited electronic states to the total ME spectrum will decrease with the separation of the respective electronic state from the CEF ground state. Since various lines superpose, the resulting ME spectrum will *not* be strictly polarized in general.[7] It should be noted that the case of slow relaxation processes discussed here differs from the fast relaxation case, where an external magnetic field produces an *averaged* effective hf field, which results in a polarized ME spectrum.[23] Since the direct contribution of the external magnetic field to the hf splitting is negligibly small in the source ($H_{eff}\gg H$) and in the absorber,[45] the splitting of the ME spectrum in the static limit is given by Eq. (5). The quadrupole interaction given by Eq. (6) will shift the $\Delta I_z=\pm1$ lines by $-3BQ_i$ (compare Table I). The static-limit line positions and the static-limit line width of 3.9 mm/sec will then be altered by the relaxation processes. Since all parameters for the static limit are known the change of the Mössbauer spectrum with field and temperature is simply dependent on the relaxation effects determined by the $4f$–conduction-electron coupling. In the following we will discuss the experimental spectra and their analysis.

B. Spectra and their analysis

Experimental results at 4.2 K and for external fields between 10 kG and 55 kG are shown in Fig. 2. The solid lines through the data points represent a least-squares fit using the microscopic relaxation theory described above. In the analysis we have allowed for a generalized Schrieffer-Wolff interaction, a frequency dependent spectral density, and an equal initial population of all eight electronic energy levels of the free-ion ground state $^2F_{7/2}$. In the fitting procedure the values $A=4.55$ mm/sec, $B=0.125$ mm/sec, and $\Gamma_{min}=3.9$ mm/sec were used. The CEF parameters $x=0.77$ and $W=3.65$ K were taken from Ref. 16. The electronic Stark and Zeeman energies E_i and the corresponding wave functions ψ_i were obtained from Eq. (1) for the various external fields H and the three directions [001], [111] and [110]. For each direction the two static-hf frequencies ($\Delta I_z=\pm1$) were calculated according to Eq. (8) and used to obtain the relaxation Mossbauer spectrum [Eq. (36)], which then only depended on a single free parameter $|I_c\rho(E_F)|^2$. Finally, the total averaged ME spectrum was obtained according to Eq. (9). The four spectra in Fig. 2 could be uniquely fitted with a value of $|I_c\rho(E_F)|^2=(9.0\pm1.0)\times10^{-4}$ for the coupling strength. Mössbauer spectra taken in the temperature range 4.2 to 40 K and with an external magnetic field of 50 kG are shown in Fig. 3. The solid curves through the data points were calculated with the same parameters that were used for the spectra of Fig. 2. However, in this case the field was fixed and the temperature varied. The value for the coupling strength deduced from this data is also $(9.0\pm1.0)\times10^{-4}$.

IV. DISCUSSION

In a complex problem with relaxation processes between various states the definition of a single

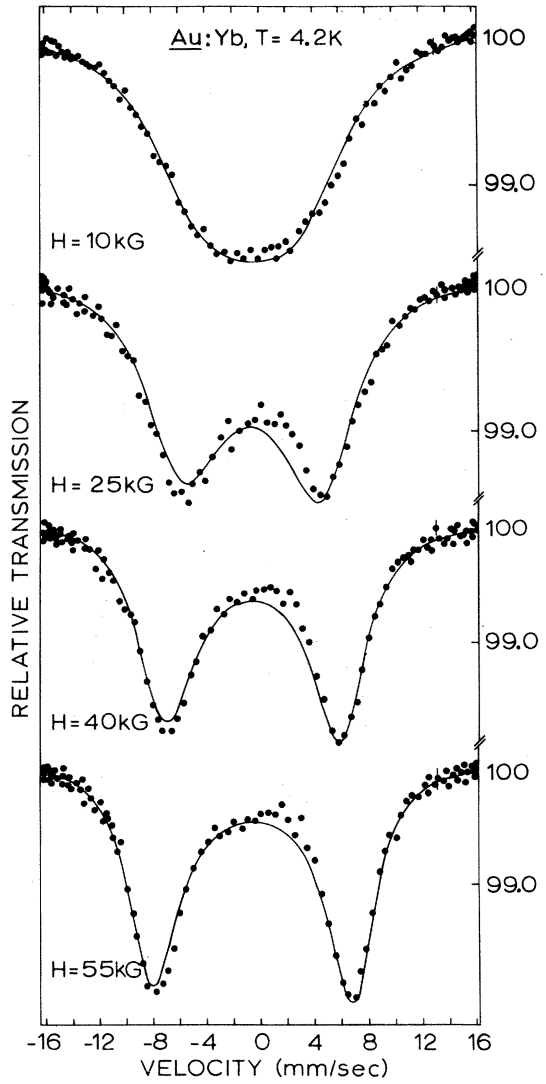

FIG. 2. Mössbauer-relaxation spectra of Yb impurities in Au at $T=4.2$ K and in various external magnetic fields H. The theoretical curves were calculated with the experimental values for T and H, $A=4.55$ mm/sec, $B=0.125$ mm/sec, $\Gamma_{\min}=3.9$ mm/sec, $x=0.77$, and $W=3.65$ K. A least-squares fit yielded $|I_c\rho(E_F)|^2 = (9.0\pm1.0)\times10^{-4}$ for all spectra. Positive velocities correspond to positive hf energies (eigenvalues of Eq. (8)].

"relaxation rate" is no longer reasonable since various relaxation rates exist and the rates may differ by orders of magnitude. The shape of the relaxation ME spectrum produced by a specific electronic state is then determined by the fastest rate with which this level relaxes to any other level. Furthermore, when the relaxation rate ω_R is increased from the static limit there is relaxation broadening in the ME in the slow relaxation regime $\omega_R \ll \omega_{hf}$ and relaxation narrowing in the fast relaxation regime $\omega_R \gg \omega_{hf}$.

As seen from Fig. 1 and Table I the two lowest levels of Yb in Au are separated by less than 13 K for external fields up to 55 kG, while the other six levels are always between 75 and 100 K above the ground level. The decay relaxation rates at $T=4.2$ K of the six excited states to the ground state [Eq. (35)] are always found to decay quickly ($|\bar{R}_{61}| \gtrsim 150$ mm/sec) while the second-lowest state has a decay rate of the order of 15 mm/sec or less. Since at 4.2 K the upward transitions to the six highest states are negligible ($|\bar{R}_{16}| \leq 0.5$ mm/sec) the spectra shown in Fig. 2 may be discussed in terms of relaxation processes between the lowest two electronic levels only. It should be noted that

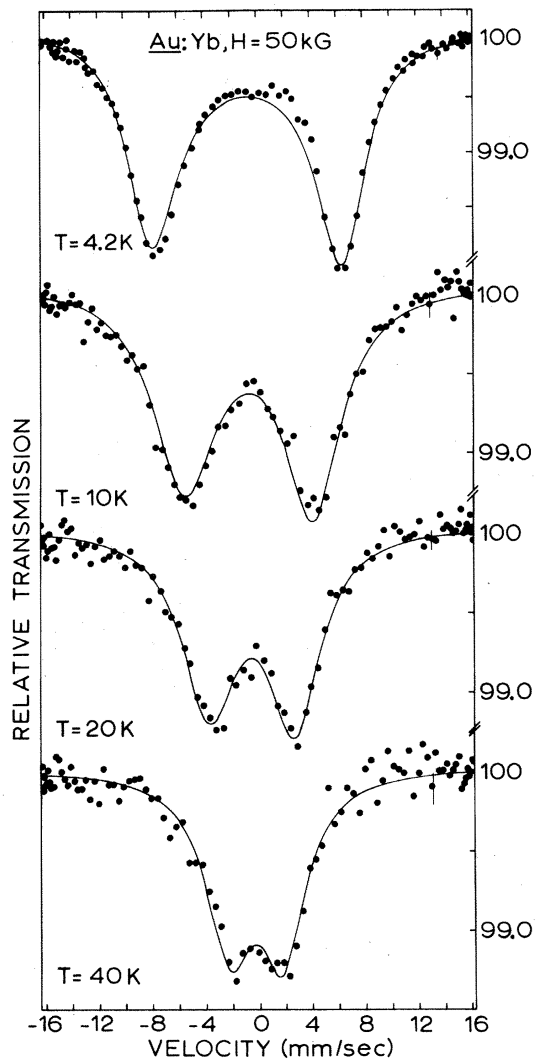

FIG. 3. Mössbauer-relaxation spectra of Yb in Au in a magnetic field $H=50$ kG and at various temperatures T. The theoretical curves were calculated with the experimental values for H and T and the parameters used for Fig. 2. Again $|I_c\rho(E_F)|^2=(9.0\pm 1.0)\times10^{-4}$ could account for all spectra. Velocity convention as in Fig. 2.

TABLE II. Static-limit magnetic and quadrupole splittings [compare Eqs. (5) and (6)] for the $\Delta I_z = \pm 1$ lines at various fields $\vec{H} \parallel [001]$, assuming $A = 4.55$ mm/sec, $B = 0.125$ mm/sec, $x = 0.77$, and $W = 3.65$ K.

		Field (kG)			
	Level	10	25	40	55
Magnetic	2	±6.6	±6.1	±5.6	±5.1
Splitting (mm/sec)	1	±7.1	±7.4	±7.8	±8.1
Quadrupole	2	0.07	0.18	0.29	0.41
Shift (mm/sec)	1	−0.06	−0.15	−0.23	−0.30

the analysis of our previous measurements in weak external fields at 1.4 and 4.2 K (Ref. 7) remains unchanged for this very reason.

Contrary to the situation in $YbPd_3$,[23] where the hf field shows a Brillouin type of behavior due to fast electronic relaxation at zero field, in the case of Yb impurities in Au relaxation rates at zero field and 4.2 K are already slower (6.65 mm/sec) than $\omega_{hf} \approx 15$ mm/sec.[7] Thus a change in hf splitting of Yb impurities in Au is solely due to admixing of the CEF wave functions by the applied field. In Table II we have listed the calculated hf splittings (corresponding to the $\Delta I_z = \pm 1$ transitions) produced by the two lowest electronic states in various external fields along [001]. The magnetic hf splittings are seen to slightly increase for the ground state (level 1) and decrease for the first excited state (level 2) with increasing field. The quadrupole splitting for both states is found to increase with field (note opposite signs in Table II) owing to stronger admixing at higher fields. However, this increase in the total hf splitting cannot solely account for the drastic change in the spectra between 10 and 55 kG.

On the other hand, we have listed in Table III the relaxation rates R_{ij} between the lowest two states at $T = 4.2$ K. The dependence of the relaxation rates on field as shown in Table III is due to the increasing splitting of the lowest two states with field. This splitting is nearly linear for fields up to 55 kG and increases at an approximate rate of 2.3 K per 10 kG. At 10 kG the up (R_{12}) and down (R_{21}) rates are still comparable and the relaxation broadening for which the rates R_{ij} are a measure is about two times the static-limit width (3.9 mm/sec) and about half of the total hf splitting (≈ 13.7 mm/sec; compare Table II). Thus the two hf spectra of the two electronic states are not resolved and one sees a broad central intensity. At 55 kG we see that $|R_{21}| \gg |R_{12}|$ and thus the upper state does not contribute greatly to the hf spectrum, which is then basically determined by the ground level. This ground level relaxes very slowly ($R_{12} \approx 1$ mm/sec) to the upper state and its hf structure is thus well resolved. The experimental asymmetry in the spectrum at 55 kG (compare Fig. 2) is accounted for by the quadrupole interaction of the ground level. From Table I it is seen that the quadrupole shift ($-3BQ_i$) is negative for the ground state and in addition shows a directional dependence which when averaged leads to the observed asymmetry. The averaging procedure [compare Eq. (9)] is therefore indeed necessary for the problem at hand.

It is important to note that the contribution of the first excited state does not vanish at 55 kG. In Fig. 4 we have simulated two spectra with the parameters used to fit the 55 kG spectrum in Fig. 2. In one case (dashed curve) we have assumed an initial Boltzmann population as would be correct for an absorber experiment, in the other case an equal initial population of the two lowest energy levels is assumed as is appropriate for source experiments. Our experimental data clearly favor the second simulation and thus provide experimental evidence for our previous theoretical considerations on rearrangement in Mössbauer-source experiments. As has been pointed out at the end of Sec. II D, rearrangement has formally been treated by assuming a unit density matrix W in the expression of the Mössbauer spectrum appropriate for an absorber. The successful fitting of the spectra in Figs. 2 and 3 indicates that this approach is not too bad an approximation. It should be pointed out that attempts to fit the spectra by assuming a Boltzmann intial population were less successful. In this case the basic problem was that no set of values for the hf coupling constants A and B could uniquely account for all spectra.

At 50 kG the electronic energies and wave functions (and in turn the static-limit hf splittings) are fixed and the change in the spectra of Fig. 3 with temperature is solely due to changes in the relaxation rates. In particular, within our relaxation theory only the exponential factor in Eq. (35) changes. While the relaxation rates generally increase with temperature, as seen from Eq. (35), it is especially the upward transition rates which become more probable. In Table IV we have listed the relaxation rates in the ground doublet (R_{12})

TABLE III. Relaxation rates in the ground doublet at various fields and $T = 4.2$ K. We have assumed $x = 0.77$, $W = 3.65$ K and a tensor-type coupling with $|I_c \rho(E_F)|^2 = 9 \times 10^{-4}$.

Field (kG)	$\|R_{12}\|$ (mm/sec)[a]	$\|R_{21}\|$ (mm/sec)[a]
10	5.5	9.5
25	3.4	13.4
40	1.7	15.3
55	1.2	22.9

[a] 1 mm/sec = 67.96 MHz = 426.93×10^6 sec^{-1}.

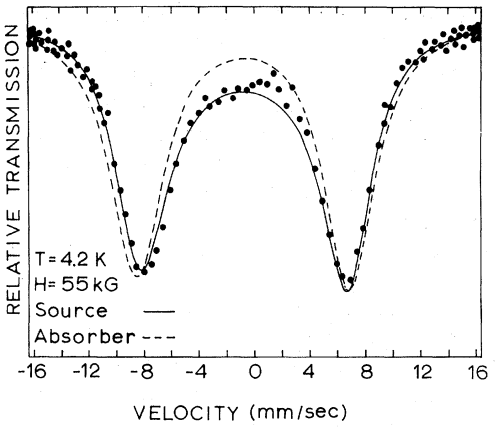

FIG. 4. Simulated Mössbauer spectra for the case of a source and a hypothetical absorber experiment of *Au*: Yb at $T=4.2$ K and $H=55$ kG. The solid (source) curve is identical to the curve through the data points at 4.2 K and 55 kG in Fig. 2.

and an averaged upward and downward rate between the ground state and the group of the six uppermost levels ($\bar{R}_{16}$). The steep relative increase of R_{12} with temperature results in a larger relative intensity contribution of the first excited state to the hf spectrum. Furthermore, the hf structure of the ground state will no longer be static.

At 50 kG and 10 K the average relaxation rate (≈ 20 mm/sec) is already slightly larger than ω_{hf}, indicating that we have entered the relaxation-narrowing regime. This case should be contrasted to the ME spectrum at 4.2 K and 10 kG, where severe relaxation broadening is encountered. The effect of relaxation narrowing on the ME spectrum is very nicely seen at the highest temperature of 40 K. The spectrum has collapsed considerably. In the temperature range 10–40 K the upward transitions from the lowest two levels to the uppermost six levels are found to have a finite probability (compare Table IV). However, since we are in the fast relaxation regime, additional contributions to the relaxation rates within the ground doublet (e.g., via Orbach type processes) are not easily separable experimentally. On the other hand, the probabilities for the decays are still at least a factor of 7 larger than for the excitations. This is why the uppermost six states do not greatly contribute in intensity to the ME spectrum.

The temperature dependence of the hf splitting as displayed in Fig. 3 has some analogy to earlier studies of $YbPd_3$,[23] where a Brillouin type of behavior for the hf field was observed. At higher temperatures (10–40 K) for the *Au*:Yb system we are also in the range of fast electronic relaxation and thus the hf field shows saturation effects. If we consider the hf splitting in Fig. 3 as a function of H/T we clearly see that the hf splitting increases with H/T, as is the case for $YbPd_3$. The fact that the experimental data are well described by the theory which assumed a definite set of CEF parameters (i.e., those of Ref. 16) is then a direct consistency check for the same.[23] Our data, however, are not sensitive enough to determine the absolute values of the CEF parameters more precisely than the susceptibility data.[16,17]

Our experimental results do not provide a sensitive check of whether the $4f$–conduction-electron coupling should be described by a vector exchange or a general tensor-type coupling. Since the wave functions ψ_i are a linear combination of the CEF wavefunctions, nearly all transitions between the $2J+1$ states are allowed, even by the vector exchange. The Γ_6 and Γ_8 wave functions are especially strongly admixed because of the small CEF splitting between these levels. Therefore even the Zeeman levels of the Γ_6 state can decay to the Γ_7 ground doublet, which for a vector exchange is not possible in the zero-field case.[8] In principle it is already clear from previous ME studies, especially from the study of ^{166}Er in dilute *Au*:^{166}Ho sources[4] without external fields, that a general tensor type of coupling is better suited, since under the assumption of a vector exchange one would expect significant contributions to the ME spectrum from the Γ_6 state.[8] For the particular case of *Au*:Yb there is another reason why the generalized Schrieffer-Wolff coupling should be used. Since the $4f^{14}$ closed-shell configuration is close to the $4f^{13}$ ground configuration[33] the magnitude of $E_{exc}^{(+)}$ is small. For this reason, the generalized Schrieffer-Wolff coupling is expected to be the dominant source of the $4f$–conduction-electron coupling (compare Eq. 14). It should be noted that the occurence of a magnetic moment on Yb impurities in Au means that $E_{exc}^{(+)}$ is still considerably larger than the virtual bound-state width, and it is thus justifiable to treat the $4f$–conduction-electron coupling in perturbation.[26]

Finally, the Kondo problem needs to be briefly discussed. Resistivity studies[12] indicate that *Au*:Yb is a Kondo system. In previous ME studies

TABLE IV. Relaxation rates in the ground doublet (R_{12}) and between the ground state and the uppermost group of levels ($\bar{R}_{16}$) at various temperatures and $H=50$ kG. The parameters are as for Table III.

T (K)	$\lvert R_{12}\rvert$ (mm/sec)[a]	$\lvert R_{21}\rvert$ (mm/sec)[a]	$\lvert \bar{R}_{16}\rvert$ (mm/sec)[a]	$\lvert \bar{R}_{61}\rvert$ (mm/sec)[a]
4.2	1.4	22	0	150
10	9	29	<0.1	150
20	26	46	2	152
40	60	80	19	153

[a] 1 mm/sec = 67.96 MHz = 426.93×10^6 sec^{-1}.

of Yb impurities in Au (Ref. 13) a weak anomaly in the relaxation rate has been reported. This has been associated by the authors[13] with the Kondo effect. In order to see whether a change in the coupling strength occurs[46] when the zero-field and high-field data at 4.2 K are compared, we have reanalyzed our previous data[7], assuming a generalized Schrieffer-Wolff coupling.[30] This analysis yielded $|I_c\rho(E_F)|^2 = (8.5 \pm 0.5) \times 10^{-4}$ for the coupling strength, which is within error bars of the value derived for the data taken with field. Indeed, in evaluating systems with a Kondo temperature as low as 10 mK or less[13] the error bars of the physical parameters are very significant, since the Kondo contribution is small. For example, comparing the values and error bars for the coupling strength as determined with and without field a change of up to 20% is possible without being discovered experimentally. It appears that our measurements are not sensitive enough to yield information on the Kondo effect.

ACKNOWLEDGMENTS

The author would like to thank Dr. L. L. Hirst not only for numerous helpful discussions but also for providing his results prior to publication. Collaboration at an early stage of the problem and fruitful discussions with Dr. G. K. Shenoy are gratefully acknowledged. Discussions with Professor G. M. Kalvius have also been most helpful.

[1]B. B. Schwartz and R. B. Frankel, in *Mössbauer Effect Methodology*, edited by I. J. Gruverman (Plenum, New York, 1971), Vol. VII, p. 21.
[2]L. L. Hirst, E. R. Seidel, and R. L. Mössbauer, Phys. Lett. A 29, 673 (1969); L. L. Hirst and E. R. Seidel, J. Phys. Chem. Solids 31, 857 (1970).
[3]F. Gonzalez Jimenez and P. Imbert, Solid State Commun. 11, 86 (1972).
[4]G. K. Shenoy, J. Stöhr, and G. M. Kalvius, Solid State Commun. 13, 909 (1973).
[5]J. Stöhr, W. Wagner, and G. K. Shenoy, Phys. Lett. A 47, 177 (1974).
[6]J. Stöhr and G. K. Shenoy, Solid State Commun. 14, 583 (1974).
[7]J. Stöhr, W. Wagner, G. M. Kalvius, and G. K. Shenoy, in Proceedings of the International Conference on Hyperfine Interactions Studied in Nuclear Reactions and Decay, Uppsala, June 1974 (unpublished); G. K. Shenoy, J. Stöhr, W. Wagner, G. M. Kalvius, and B. D. Dunlap, Solid State Commun. 15, 1485 (1974).
[8]L. L. Hirst, J. Stöhr, G. K. Shenoy, and G. M. Kalvius, Phys. Rev. Lett. 33, 198 (1974); 33, 1463E (1974).
[9]J. Stöhr, G. M. Kalvius, G. K. Shenoy, and L. L. Hirst, in Ref. 7.
[10]B. Coqblin and J. R. Schrieffer, Phys. Ref. 185, 847 (1969).
[11]L. L. Hirst, Z. Phys. 244, 230 (1971).
[12]A. P. Murani, Solid State Commun. 12, 295 (1973).
[13]F. Gonzalez Jimenez and P. Imbert, Solid State Commun. 13, 85 (1973); and in Proceedings of International Conference on Magnetism, Moscow, August 1973 (unpublished).
[14]R. B. Frankel, N. A. Blum, B. B. Schwartz, and D. J. Kim, Phys. Rev. Lett. 18, 1051 (1967).
[15]K. R. Lea, M. J. M. Leask, and W. P. Wolf, J. Phys. Chem. Solids 23, 1381 (1962).
[16]G. Williams and L. L. Hirst, Phys. Rev. 185, 407 (1969).
[17]A. P. Murani, J. Phys. C Suppl. 2, 153 (1970).
[18]L. J. Tao, D. Davidov, R. Orbach, and E. P. Chock, Phys. Rev. B 4, 5 (1971).
[19]M. T. Hutchings, Solid State Phys. 16, 277 (1966).
[20]S. Ofer, I. Nowik, and S. G. Cohen, in *Chemical Applications of Mössbauer Spectroscopy*, edited by V. I. Goldanskii and R. H. Herber (Academic, New York, 1968), p. 427.
[21]L. L. Hirst, Z. Phys. 245, 378 (1971).
[22]R. E. Watson, P. Bagus, and A. J. Freeman, Bull. Am. Phys. Soc. 13, 482 (1968).
[23]I. Nowik, B. D. Dunlap, and G. M. Kalvius, Phys. Rev. B 6, 1048 (1972).
[24]Throughout this paper we will use the units mm/sec for the Mössbauer hf-splitting energy as well as for the relaxation rate, since both need to be compared in the discussion of relaxation effects. For ^{170}Yb the conversion 1 mm/sec = 67.96 MHz = 426.93×10^6 sec^{-1} holds.
[25]J. R. Schrieffer and P. A. Wolff, Phys. Rev. 149, 491 (1966); J. R. Schrieffer, J. Appl. Phys. 38, 1143 (1967).
[26]L. L. Hirst, Phys. Kondens. Mater. 11, 255 (1970).
[27]P. W. Anderson, Phys. Rev. 124, 41 (1961).
[28]A. Narath, Phys. Rev. 163, 232 (1967).
[29]L. L. Hirst, Adv. Phys. 21, 759 (1972).
[30]L. L. Hirst (unpublished).
[31]A. R. Edmonds, *Angular momentum in quantum mechanics* (Princeton U. P., Princeton, N.J., 1957).
[32]A. J. Heeger, Solid State Phys. 23, 283 (1969), see especially p. 295.
[33]For many other systems rearrangement is considerably slower than for *Au*:Yb. In the present case the excited $4f^{14}$ closed shell configuration is close to $4f^{13}$ (see for example Ref. 12). Because of the anomalously small value of $E_{\rm exc}^{(+)}$ [compare Eq. (14)] the coupling constant I_c is large and hence rearrangement is fast for *Au*:Yb.
[34]L. L. Hirst, J. Phys. Chem. Solids 31, 655 (1969).
[35]The correlation function $G(t)$ is defined differently in Ref. 34. We feel that the approach used here is the more convenient and natural formalism.
[36]The frequency is included with the wrong sign in the definition of the spectral density, Eq. (5) of Ref. 34. Thus, Hirst's equation (4) differs from Eq. (25).
[37]Equation (28) differs slightly from Eq. (8) in Ref. (34) owing to a different definition of the correlation function $G(t)$. However, the two formulations are identical if the relaxation matrix R in Eq. (8) of Ref. (34) is taken to be the transpose of the relaxation matrix defined here.
[38]H. H. Wickman, in *Mössbauer Effect Methodology* (Plenum, New York, 1966), Vol. II.
[39]A. J. F. Boyle and H. E. Hall, Rep. Prog. Phys. 25, 411 (1962).

[40] *Table of isotopes*, edited by C. M. Lederer, J. M. Hollander, and I. Perlman (Wiley, New York, 1967).

[41] For an arbitrary nuclear transition $I \rightarrow I'$, $\vec{\epsilon}_n$ must be calculated according to Eq. (30). Since the index n denotes a fixed set of nuclear quantum numbers I_z and I'_z, the vector $\vec{\epsilon}_n$ is just a unit vector multiplied by the respective Clebsch-Gordan coefficient $\langle I', I'_z, k, q | I, I_z \rangle$.

[42] For a review see, for example, H. Schwegler, Fortschr. Phys. 20, 251 (1972).

[43] F. Gonzalez Jimenez, P. Imbert, and F. Hartmann-Boutron, Phys. Rev. B 9, 95 (1974); B 10, 2143E (1974).

[44] H. Maletta, K. R. P. M. Rao, and I. Nowik, Z. Phys. 249, 189 (1972).

[45] E. E. Havinga, K. H. J. Buschow, and H. J. van Daal [Solid State Comm. 13, 621 (1973)] found that Yb in $YbAl_3$ is ambivalent. In $YbAl_3$ the separation between the ground ($4f^{14}$) and first-excited ($4f^{13}$) configuration is very small. As is seen from Eq. (14), in such a case the relaxation rates in the electronic shell of Yb are extremely fast. In addition the large conduction-electron density of states at the Fermi surface in $YbAl_3$ (found by Havinga *et al.*) increases the relaxation rates. Since isomer shifts for the ^{170}Yb isotope are also negligible, $YbAl_3$ is a Mössbauer absorber with a single narrow line. Even under application of magnetic fields the hf structure of the electronic shell is expected to average to zero because of fast relaxation (the splitting $2g_N\mu_N H$ due to the external field is unmeasurably small). This is in agreement with experimental results for fields up to 50 kG and in the temperature range 4.2–100 K [G. K. Shenoy and B. D. Dunlap (private communication)].

[46] A change in the coupling strength $|I_c\rho(E_F)|^2$ would be solely due to a change in I_c since the conduction-electron density of states per spin direction, $\rho(E_F)$, is unchanged for the field strengths used in this study.